SCIENCE CHINA
Information Sciences

• RESEARCH PAPER •

July 2022, Vol. 65 172204:1–172204:15
https://doi.org/10.1007/s11432-021-3476-9

Complex network approach for the evaluation of asphalt pavement design and construction: a longitudinal study

Hanjie LIU[1,2], Jinde CAO[1,2*], Wei HUANG[3], Xinli SHI[4] & Xudong WANG[5]

[1]*School of Mathematics, Southeast University, Nanjing* 210096*, China;*
[2]*Jiangsu Provincial Key Laboratory of Networked Collective Intelligence, Southeast University, Nanjing* 210096*, China;*
[3]*Intelligent Transportation System Research Center, Southeast University, Nanjing* 210096*, China;*
[4]*School of Cyber Science and Engineering, Southeast University, Nanjing* 210096*, China;*
[5]*Research Institute of Highway Ministry of Transport, Beijing* 100088*, China*

Received 27 August 2021/Revised 24 November 2021/Accepted 2 March 2022/Published online 20 June 2022

Abstract The assessment of asphalt pavement structures with diversified designs and constructions has been a critical challenge due to the practical limitations in testing and methodology. Here, we propose a complex network approach to the evaluation of longitudinal asphalt pavement performances in the Research Institute of Highway Ministry of Transport track (RIOHTrack). We add to the growing field in which network approaches are employed and indicate the profound application in understanding pavement structures. Specifically, similar and disparate pavement performances are revealed regardless of their predefined design and construction categories. Evidence shows that short-term pavement performance depends on the strength of the subbase structure, whereas long-term performance relies on the thickness of the asphalt layer. In addition, our results indicate that recycling materials could be an important substitute for reducing the thickness of asphalt concrete and maintaining a healthy service life.

Keywords complex network, asphalt pavement, structure evaluation, longitudinal, RIOHTrack

Citation Liu H J, Cao J D, Huang W, et al. Complex network approach for the evaluation of asphalt pavement design and construction: a longitudinal study. Sci China Inf Sci, 2022, 65(7): 172204, https://doi.org/10.1007/s11432-021-3476-9

1 Introduction

An important goal in the study of pavement structures is the establishment of long life asphalt pavement, the goal of which requires continuous development in material innovation, production, maintenance management, and systematic evaluation of pavement performances. The concept of long life pavement is introduced in the past decades in America and Europe, and it aims to provide a low life-cycle cost and resource consumption [1]. The design and construction of long-life pavements are based on early concepts, such as deep-strength, stage-by-stage, and full depth asphalt base structure, but differ in exploring more advanced pavement materials and functionality. In practice, the intention of long life pavements is to extend the existing pavement performance by restricting distress such as fatigue and cracking, but theoretically, by completely eliminating these phenomena [2].

The assessment of pavement performance has been a challenging issue in the literature due to the time course of the assessment, multivariate nature of influencing factors, and diversified pavement structure design and construction [3]. Previous studies focused on the in-situ monitoring of pavement performance under real-world traffic or laboratory simulations [4–6]. However, there is a significant variation in the selected time duration of the assessment period, which ranges from 5 to 50 years. Intuitively, some pavement structures may not show superior performance at the beginning of their service life, but they may maintain a healthy life for a longer time than others. Thus, cross-sectional studies, which assess

* Corresponding author (email: jdcao@seu.edu.cn)

the pavement performance in a period of time, could overlook factors that might not have an impact on pavement structures [7]. Subsequently, results are biased in terms of the long-term effect.

Moreover, a host of studies have indicated multiple profound influencing factors that are correlated with the pavement life service, and several pavement measurements have been demonstrated to reflect critical pavement performances. Specifically, temperature and moisture-related factors have been widely recognized to have significant impacts on pavement structures, subsequently affecting the response of pavement performance [8]. Particularly, the behavior of the asphalt concrete (AC) layer heavily depends on the change in temperature. For instance, the modulus value of AC materials increases in low-temperature conditions, whereas an opposite pattern emerges in high-temperature conditions [9]. This phenomenon is much in line with the seasonal variations of pavement performance. Studies showed dramatic changes in the load-carrying capacity of pavements in cold winter and different structure designs could have different performance responses [10, 11].

Furthermore, pavement performance is reflected in various tests, among which the rutting depth (RD), texture depth (TD), and international roughness index (IRI) have been demonstrated as critical indicators of pavement health. Rutting results in permanent, irreversible residual strain in asphalt pavements, and it directly reflects the pavement health condition [12]. The TD of the pavement is closely related to the skid resistance [13], which depicts the friction resistance between a vehicle tire and pavement surface, and is responsible for noise emission [14]. Lastly, the IRI is a characteristic that measures pavement roughness conditions, and it has been shown to predict distress, such as transverse cracking, rutting, and fatigue [15]. Those measurements play an essential role in pavement evaluation and maintenance decision makings.

Almost all elements of major pavement designs are not by any means new. Some have been circulating in different forms. For instance, full-depth AC pavements are composed of a relatively thick AC layer directly constructed upon the subgrade base, but with a relatively thinner total depth of the pavement structure as compared with conventional AC pavements. Studies showed superior performance of full-depth AC in loading capacity than the standard AC structure [16] and showed stable performance in a 10-year longitudinal study [17]. A similar comparison was performed between inverted and flexible pavements. Under the same loading condition, an inverted structure experiences a low tension and small surface deflection [18]. Moreover, the RD of varied semi-rigid base pavements was evaluated, and the results show that different bottom base material impacts the rutting resistance [19]. Nonetheless, in the literature so far, studies have focused on the comparison and assessment of pavement structures within a small set of a certain design category due to the practical limitations in experiments and methodology concerns [20].

Traditional laboratory experiments have a limited number of pavement structures that are tested at the same time under the same condition, which merely imitates real traffic conditions [21]. To simultaneously capture the lifelong performance characteristics of multiple pavements, a full-scale field accelerated pavement testing, which mimics degradations induced by real traffic accumulated during the lifetime of a pavement structure in a short period of time, is proposed [22]. The method offers a large sample of data to probe the performance of pavement. However, studies in the literature largely relied on correlation and regression methods for the investigation of influencing factors on the pavement performance [23, 24]. Another line of research focuses on finite element analysis to understand the behavior of pavement substructures under load [25, 26]. Those methods are constrained in handling high-dimensional data and limited in delivering evaluation of pavement performances on a broad scale.

In the current study, we propose a complex network approach for the evaluation of a large set of pavement structures from several design categories in a full-scale accelerated loading experiment. Network science, stemming from social networks, has been adopted by various research disciplines to address problems that involve multidimensionality with many objects. It offers a window to examine the complexity of the relationship brought from high dimensionality. Consequently, it has become possible to explicitly investigate many pavement performances in parallel. In this study, we constructed an accelerated pavement loading testing field located in Beijing, which contains 19 pavement structures from six major design categories, and tested it over the past four years (i.e., 2017–2020). The longitudinal nature of the data would provide important insights into the pavements' short- and long-term performances. Furthermore, we expect to search for a data-driven categorization of pavement design and construction, such that structures from a certain design category may have a similar performance or service life with those that have a completely different design and construction.

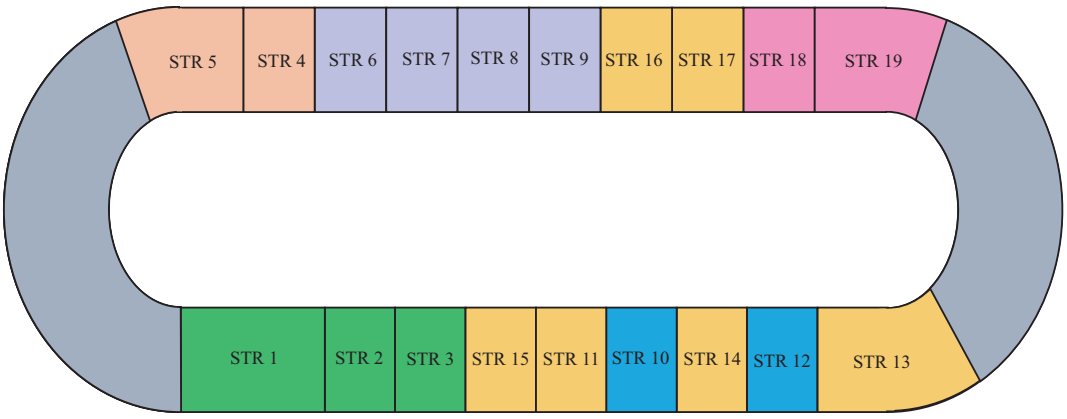

Figure 1 (Color online) Schematic overview of the RIOHTrack testing field. Colors represent the different predefined design categories shown in Table 1. STRs 1–3 highlighted in green color refer to the thin AC semi-rigid base structure, and structures on the circular curve are omitted.

Table 1 Designed categories of asphalt pavements in RIOHTrack

	Category	Pavement
I	Thin AC semi-rigid base structure	STRs 1–3
II	Common semi-rigid base structure	STRs 6–9
III	Rigid composite base structure	STRs 4 and 5
IV	Inverted structure	STRs 10 and 12
V	Thick AC base structure	STRs 11, 13–17
VI	Full depth AC structure	STRs 18 and 19

2 Methodology

2.1 Full-scale track testing

The Research Institute of Highway Ministry of Transport track (RIOHTrack), located in Beijing (39.9°C north latitude), is a field full-scale accelerated pavement testing road designed for long-term field performance and evaluation. The RIOHTrack is a 2.038 km-long oval with two lanes. The inner lane is designated as the carriageway, and the outside lane is the passing lane. The radius of the circular curve on the north and south sides of the track is 130.5 m with a 7% elevation slope. The designed driving speed for the track is 50 km/h, and it has a loading capacity of 10 million equivalent single axle load (ESAL) per year. The schematic overview of the testing field is shown in Figure 1.

The RIOHTrack includes 25 types of asphalt pavement structures, i.e., 19 main testing structures on the straight line and 6 anti-rutting material sections on the circular curve. In the current study, we focus on the evaluation of structures on the straight line, labeled as STRs 1–19. The total thickness of each pavement structure is in the range of 68–100 cm, consisting of an asphalt layer with a minimum thickness of 12 cm to a maximum thickness of 52 cm. The designed pavement structure can be further divided into six categories according to the structure combination and thickness of the asphalt layer, as shown in Table 1. The detailed architecture of the designed pavement structures is displayed in Figure 2 and can be found in our previous study [27].

In this study, we focus on periodical testing measurements conducted after each 20–30 thousand kilometers, including the RD, TD, and IRI. The pavement RD was measured using two detection tools: an artificial three-meter ruler and a laser profilometer. The pavement TD was detected by an eight-wheel instrument and bump accumulation instrument. Finally, the IRI was computed with a standard procedure using a quarter-car math model.

2.2 Network construction

Networks were constructed by representing each type of pavement structure on a straight line as nodes. Edges were established between two pavement structures based on the similarity of pavement performance. The network can be modeled as a graph $G(V, E, W)$, where V denotes the set of nodes or vertices, and $E \subseteq V \times V$ represents the set of edges, with W denoting the set of weights on the edge that refers to

Figure 2 (Color online) Schematic overview of the pavement structures [28]. AC: asphalt concrete; CBG-A: cement bond graded stone (7 d unconfined compression strength is 6 MPa); CBG-B: cement bond graded stone (7 d unconfined compression strength is 4.5 MPa); CS: cement soil (7 d unconfined compression strength is 2 MPa); LCC: lean cement concrete (7 d unconfined compression strength is 8 MPa); CC: cement concrete; GB: graded broken stone.

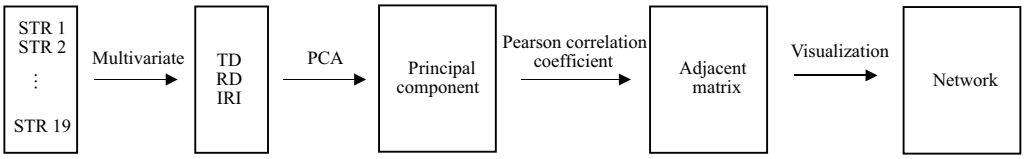

Figure 3 Schematic diagram of the network construction.

the magnitude of similarity. Four such networks were constructed based on the pavements' performances over the four years of experiments. Specifically, we performed the principal component analysis (PCA) on the data of each pavement structure. The PCA tasks are to extract the main information embedded in the pavement performance, express it using principal components, and reduce the dimensionality of data while preserving the most valuable features.

Let A be the dataset of m observations of n vector variables (i.e., $A \in \mathbb{R}^{m\times n}$). We define $C \in \mathbb{R}^{n\times n}$ as the covariance matrix of A, i.e., $C = [c_{ij}]_{n\times n}$, where $i, j \in \{1, \ldots, n\}$, and $\mathrm{cov}(\mathrm{col}_{A_i}, \mathrm{col}_{A_j})$ refers to the covariance function evaluating columns i and j.

PCA extracts the eigenvectors and eigenvalues of C, where eigenvectors are referring to as principal components. Let $p_i \in \mathbb{R}^{m\times 1}, i \in \{1, \ldots, n\}$ and $\lambda_i \in \mathbb{R}$ be the eigenvectors and corresponding eigenvalues of the covariance matrix C, respectively. The resulting matrix $P \in \mathbb{R}^{n\times n}$, contains all $p_i, i = 1, \ldots, n$ as column vectors which are in descending order corresponds to λ_i. Each principal component in P is the linear combination of the original variables, and all components are orthogonal to one another to eliminate redundant information.

In this study, PCA was performed on the surface TD, RD, and IRI. The first principal component was extracted to represent the overall performance of the pavement. Subsequently, the Pearson correlation coefficient was computed between each pair of pavement structures and served as the edge weight in the network. Finally, the adjacent matrix of the pavement network was established. The network construction process is described in Figure 3, and the visualization of the network is displayed in Figure 4.

2.3 Community detection analysis

We expect to search for data-driven phenotypic subtypes, springing from groups of pavements structure that share a similar performance and life cycle despite the differences in architecture design. We are also looking for changes in the group allegiance of pavements over the past four years. We adopted the Louvain community detection method, which is an unsupervised machine learning technique that identifies communities within a network [29]. Compared to commonly used cluster methods in the field, the most prominent feature of the Louvain algorithm is that the number of communities is decided by

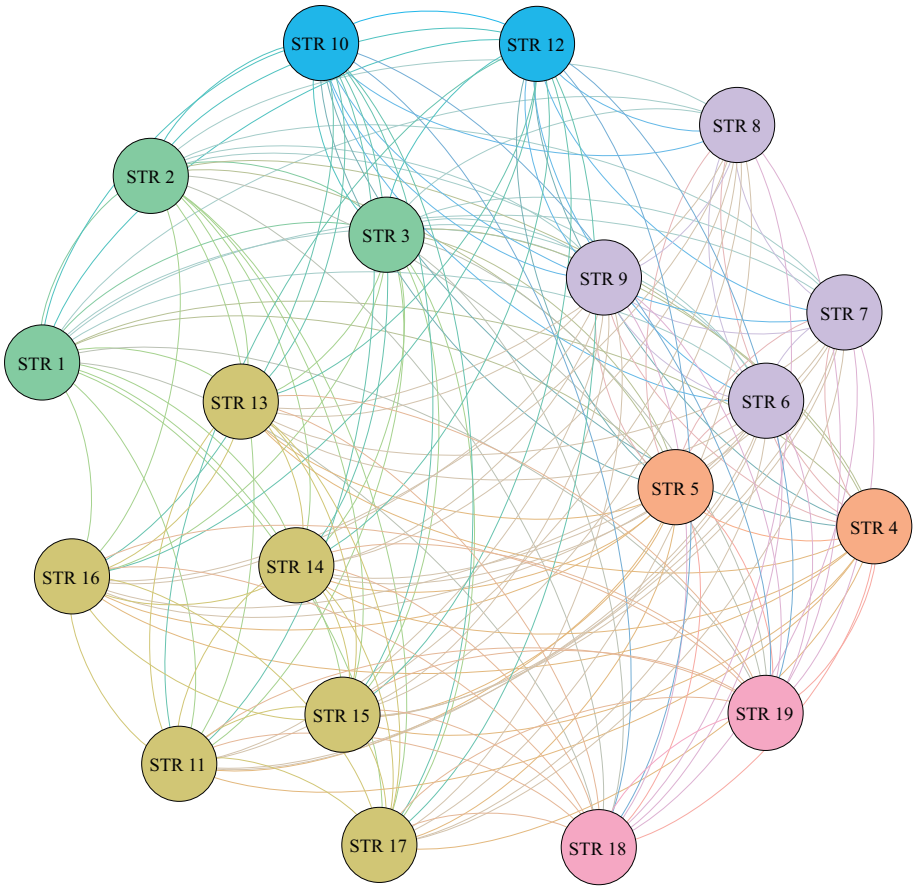

Figure 4 (Color online) Schematic overview of the constructed pavement network. Colors reflect different predefined pavement design and construction categories.

the data per se rather than by subjective decision. For instance, K-means requires an input of numbers of communities that should be derived from the data, which jeopardizes the validity of results. In the current study, we applied the community detection method to the four networks constructed based on the data from the past four years. We aimed to determine whether there exist groups of pavement structures that share a similar performance and how those groups change over the course of four years.

The greedy optimization method was used to optimize the modularity of a community in the network. The modularity (Q) is defined as the difference between the fraction of edges within a detected group and the fraction of edges in a randomized graph and is a scale ranging between -1 and 1. Formally, the modularity Q of a community C in a network $G = (V, E, W)$ is defined as follows:

$$Q = \frac{1}{2e} \sum_{i,j} \left[W_{ij} - \frac{k_i k_j}{2e} \right] \delta(g_i, g_j), \tag{1}$$

where W_{ij} represents the edge weight between nodes i and j, and k_i and k_j are the degrees of i and j (i.e., number of edges attached to i and j), respectively. e refers to the number of edges in the graph G, and δ is the Kronecker delta function; i.e., $\delta(g_i; g_j) = 1$ if $i = j$, and 0 otherwise; g_i stands for the community to which node i belongs.

The optimization processes involve the following two steps iteratively.

Step 1. Assign each node to a distinct community; that is, there are as many communities as the number of nodes. The gain of modularity for each node i is computed by selecting the largest modularity increase when moving node i into the community of each neighboring community. This process is iterated to all nodes until the modularity value stays stable.

$$\Delta_Q = \left[\frac{\Sigma_{\text{in}} + 2k_{i,\text{in}}}{2e} - \left(\frac{\sum_{\text{tot}} + k_i}{2e} \right)^2 \right] - \left[\frac{\sum_{\text{in}}}{2e} - \left(\frac{\sum_{\text{tot}}}{2e} \right)^2 - \left(\frac{k_i}{2e} \right)^2 \right], \tag{2}$$

where k_i denotes the weighted degree of node i and $k_{i,\text{in}}$ represents the weighted degree of node i in the community that i is moving into. Similarly, $\sum_{\text{in}}$ is the sum of the weights in a community, $\sum_{\text{tot}}$ is the sum of the weights attached to the node that is moving into, and $\hat{e}$ stands for the sum of the weights of all edges in the network.

Step 2. Aggregate nodes belonging to the same community and build a new network whose nodes are the communities from the previous step. Then, the first step is repeatedly performed to the new network and iterated until the modularity value becomes stable.

In the current study, the method started with initial 19 groups corresponding to 19 pavement structures. We applied the method to the four constructed networks representing the pavement structures in each of the past four years.

2.4 Statistical model and inference method

Subgroups, which were derived from the community detection analysis, were examined for differences in pavement performances over the past four years. To capture the repeated multivariate nature of the data, a bootstrapping-based repeated multivariate analysis of variance (MANOVA) was used to compare potential differences between groups in pavement performance over time. Unlike previous standard MANOVA procedures that rely on specific distributional assumptions, such as normality in multivariate or homogeneous covariance and variance between groups and in standard repeated design that assumes an equal correlation among measurements, in which those assumptions are often unrealistic in real-world data. Particularly, the number of subgroups derived from the community detection method may not be equally balanced, and repeated measurements over the years in the current study could be problematic when using traditional methods. Here, the bootstrapping strategy approach was used for the distribution of the test statistics in a robust way. This approach has been shown to provide more accurate inferential results compared to traditional methods, especially in controlling the Type-I error [30,31]. We adopt the modified ANOVA-type test statistic (MATS) with additional bootstrap for testing the main and interaction effects of factors [32]. MATS could offer the advantage of being invariant under scale transformations for multivariate data, which is an essential feature [33].

Mathematically, we consider the general linear model given by d-variate random vectors:

$$X_{gi} = \mu_i + \epsilon_{gi}, \tag{3}$$

where $i = 1, \ldots, n_g$ denote the pavement structures in group $g = 1, \ldots, a$. In this model, $\mu_g = (\mu_{g1}, \ldots, \mu_{gd})' \in \mathbb{R}^d$ is the mean vector in group $g = 1, \ldots, a$, which we aim to infer. For each g, the error term ϵ_{gi} for $i = 1, \ldots, n_g$ is presumed to be identically independent distributed d random vectors with mean $E(\epsilon_{g1}) = 0$ and variance $0 < \text{var}(X_{gi}) < \infty$. Subsequently, a null hypothesis H_0 can be formulated via contrast matrices H_μ as

$$H_0 : H_\mu = 0, \tag{4}$$

where $\mu = (\mu_1, \ldots, \mu_a)'$.

Let $\widetilde{X_\bullet} = (\widetilde{X}'_{1\cdot}, \ldots, \widetilde{X}'_{a\cdot})$ represent the vector of pooled group means $\widetilde{X}_{g\cdot} = \frac{1}{n_g}\sum_{i=1}^{n_g} X_{gi}, 1, \ldots, a$, and the estimated covariance of $\sqrt{N}\widetilde{X}$ is $\widehat{\sum_N} = N \cdot \text{diag}\{\widehat{V_1}/n_1, \ldots, \widehat{V_a}/n_a\}$. Here, $N = \sum_g n_g$ and $\widehat{V_g} = \frac{1}{n_g - 1}\sum_{n_g}^{i=1}(X_{gi} - \widetilde{X_{g\cdot}})(X_{gi} - \widetilde{X}_{g\cdot})'$. Within this framework, MATS for the testing null hypothesis is constructed as

$$M_N = M_N(X) = N\widetilde{X_\bullet}'T(T\widehat{D}_N T) + T\widetilde{X_\bullet}, \tag{5}$$

where the diagonal matrix $\widehat{D}_N = \bigoplus_{1 \leqslant g \leqslant a, 1 \leqslant i \leqslant d} N\widehat{\sigma}^2_{gi}/n_g$ of the variance $\widehat{\sigma^2_{gi}}$ of component i in group g derives an invariant under the component-wise scale transformation of MATS. The bootstrapping adaptation afterward is that MATS rejects the null hypothesis H_0 if $M_N > \hat{c}'$, where $\hat{c}'$ refers to the $(1 - \alpha)$ quantile of the distribution of the bootstrapped statistic $M'_N = M_N(X')$.

In the present study, the TD, RD, and IRI of each group measured in each year were submitted to the multivariate analysis and repeated over four seasons. Prior to the analysis, all measurements were normalized due to the different testing scales. The multivariate post-hoc analysis was conducted if the repeated MANOVA showed a significant effect after bootstrapping; otherwise, it was omitted. The multivariate post-hoc analysis would provide information with regard to the pairwise comparisons

Table 2 Comparison of the clustering quality in each year

Model	2017			2018			2019			2020		
	SC	CH	DB	SC	CH	DB	SC	CH	DB	SC	CH	DB
MS	−0.16	3.90	1.28	−0.05	3.09	1.42	−0.06	10.52	1.01	−0.03	8.66	1.23
DBSCAN	0.05	5.16	2.22	0.07	2.79	1.51	−0.13	0.34	3.00	−0.29	0.08	2.96
OPTICS	0.04	4.64	3.09	0.06	4.04	3.15	0.17	1.93	1.52	0.19	14.18	1.94
Proposed method	0.20	11.86	1.04	0.57	41.06	0.62	0.20	7.01	1.52	0.44	17.60	0.95

between four seasons. Moreover, if a significant multivariate effect was found, then the univariate pairwise comparison was performed to test the effect of individual measurements.

3 Results

We first compared the effectiveness of the complex network approach to the pavement structures with other methods. Next, the statistical analysis results of each year are presented. For clarity, only significant results are reported below. The detailed discussions of the results are presented in Section 4.

3.1 Model comparison

To validate the performance of the complex network approach, we compared it with other unsupervised clustering methods in the field. We restricted our focus to the methods that do not need the input of the number of groups, which is required in the current study. Specifically, we compared the results with the density-based spatial clustering of applications with noise (DBSCAN) [34], ordering points to identify the clustering structure (OPTICS) [35], and mean-shift clustering (MS) [36].

We adopted the commonly used index for the cluster quality evaluation. Due to the data-driven nature of this task, which does not have ground-truth labels for groups, we focused on the intrinsic measures [37]: silhouette coefficient (SC), Calinski-Harabasz index (CH), and Davies-Bouldin index (DB). SC evaluates the clustering performance based on the pairwise differences within and between group distances. The score of SC ranges from −1 to 1, where a value closer to 1 implies that the object is well matched to its own group and opposite otherwise. CH measures the validity of clustering based on the mean of the sum of squares within and between groups. A high value of CH indicates that the groups are dense and well separated. Finally, DB computes the average similarities of the mean between a group and all other groups. The smaller the value is, the better the clustering result is.

On average, the proposed complex network approach to the clustering of pavement structure performance is superior to the other methods. The detailed clustering comparisons of each of the past four years are shown in Table 2. Particularly, the proposed method displays a better mean (M) performance in the SC measurement across four years ($M = 0.35$) than MS ($M = -0.08$), DBSCAN ($M = -0.08$) and OPTICS ($M = 0.11$). Furthermore, the proposed method outperforms other algorithms in each year based on the SC measurement. In addition, the mean CH index of the proposed method is the best among the compared methods ($M = 19.38$). The MS method also shows a competitive performance in the CH index ($M = 8.66$), whereas OPTICS ($M = 6.20$) and DBSCAN ($M = 2.09$) are not performing well in the CH evaluation. Finally, the smallest DB score is revealed in the proposed approach ($M = 1.04$). Notably, the MS method has a close result ($M = 1.23$) and outperforms the proposed approach in the year 2019.

3.2 Pavement performance analysis in 2017

As expected, the subgroups derived from the clustering method were not equally balanced in each year and differed over the past four years. Specifically, in 2017, STRs 1, 4, 5, and 13 were categorized into the same group (Group 1), STRs 3, 6, 7, 12, and 14−17 belonged to the same group (Group 2), and the rest was considered as another group (Group 3). The schematic of the categorization is shown in Figure 5.

MATS after bootstrap resampling shows that the overall pavement performance diverged between the four seasons with a significant p value ($p < 0.001$), but the multivariate post-hoc comparisons did not yield any pairwise significance between any pairs of seasons. The detailed results of the post-hoc comparisons between seasons are presented in Table 3. Three groups did not differ significantly across the four seasons

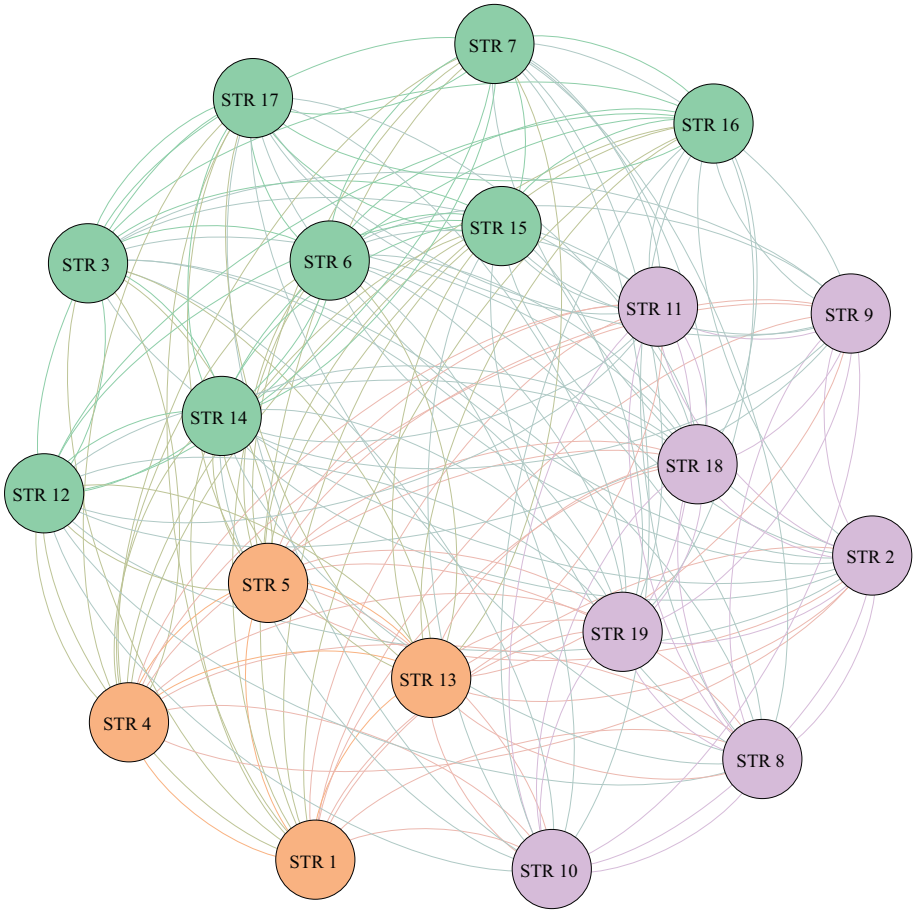

Figure 5 (Color online) Clusters from year 2017. Orange: Group 1; green: Group 2; purple: Group 3.

Table 3 p value of multivariate post-hoc comparisons between seasons[a)]

	Contrast	2017	2018	2019	2020
Summer	Spring	0.988	0.130	0.924	0.38
Fall	Spring	0.873	0.087	0.011*	0.245
Winter	Spring	0.96	0.926	0.259	0.374
Fall	Summer	0.986	0.999	0.079	0.988
Winter	Summer	0.895	0.018*	0.112	0.017*
Winter	Fall	0.669	0.006*	0.001*	0.010*

a) * refers p value < 0.05.

in the combined measurements ($p = 0.082$), although the non-significance is merely marginal. Individual measurements across the seasons in 2017 are shown in Figure 6.

3.3 Pavement performance analysis in 2018

A big change in group allegiance was observed for several pavement structures in 2018, for which two instead of three groups were derived (Figure 7). Group 1* contains STRs 1, 3–7, and 12–14, and the rest are from Group 2*. The postfix * denotes the new group to differentiate from the previous year.

The results indicate a significant difference in the combined pavement performance across the four seasons ($p < 0.001$). Multivariate post-hoc comparison reveals the significant differences in the pavement performance between winter and fall ($p < 0.05$) and between winter and summer ($p < 0.05$). Univariate post-hoc comparisons further indicate that the significance is driven from TD ($p < 0.001$), but not for the other two measures. In addition, there is a trend toward the significant seasonal effect in the pavement performance between groups in the second year of the experiment ($p = 0.084$). Individual measurements across the seasons in 2018 are shown in Figure 8.

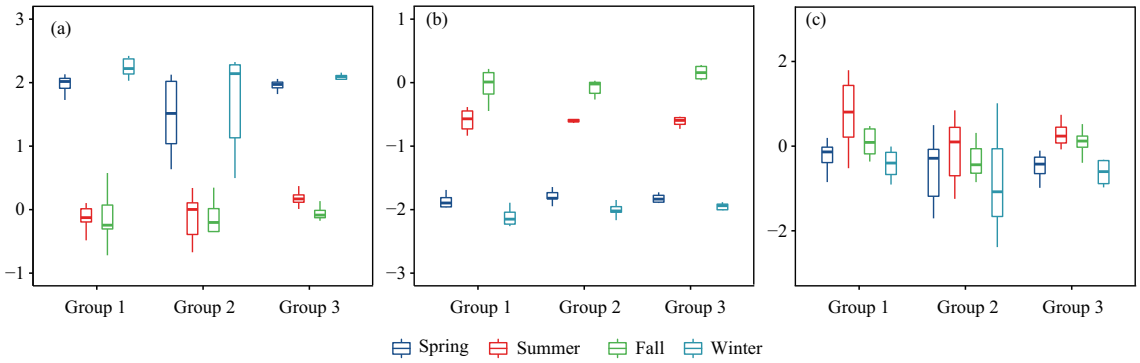

Figure 6 (Color online) Individual measurements in 2017 across seasons. (a) Texture depth across the four seasons and between groups; (b) rutting depth; (c) IRI.

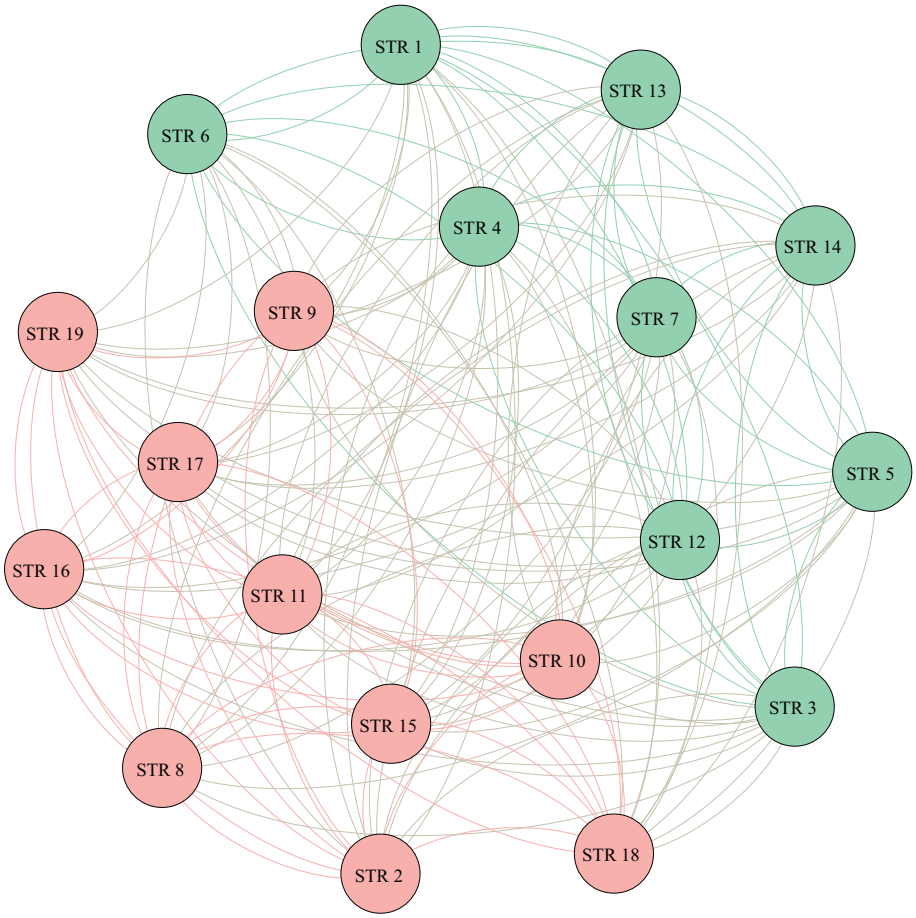

Figure 7 (Color online) Clusters of year 2018. Green: Group 1*; pink: Group 2*.

3.4 Pavement performance analysis in 2019

The community detection analysis shows a comparatively stable change of group allegiance in the third year of the experiment. STRs 7–9, 11, and 15–19 were grouped together (Group 2**), and the rest is considered as the other (Group 1**) (Figure 9). As compared to the previous year, STRs 8, 9, 11, and 15–19 stayed in the same group, whereas STRs 2, 7, and 10 changed their group affiliation.

The effect of seasonality is significant on the pavement performance ($p < 0.001$). The multivariate post-hoc comparisons show a significant difference between fall and spring ($p < 0.05$), and fall and winter ($p < 0.05$). Subsequently, the univariate post-hoc comparisons show significance underneath the RD value ($p < 0.001$). Furthermore, seasonality has a significant main effect on two groups ($p < 0.05$). Specifically, a significant difference was detected in spring ($p < 0.05$) and summer ($p < 0.05$) between the two groups,

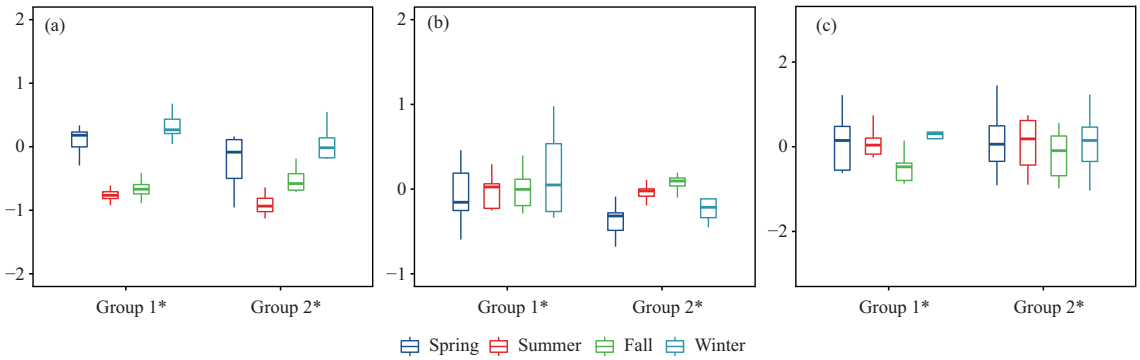

Figure 8 (Color online) Individual measurements in 2018 across seasons and between groups. (a) Texture depth across the four seasons and between groups; (b) rutting depth; (c) IRI.

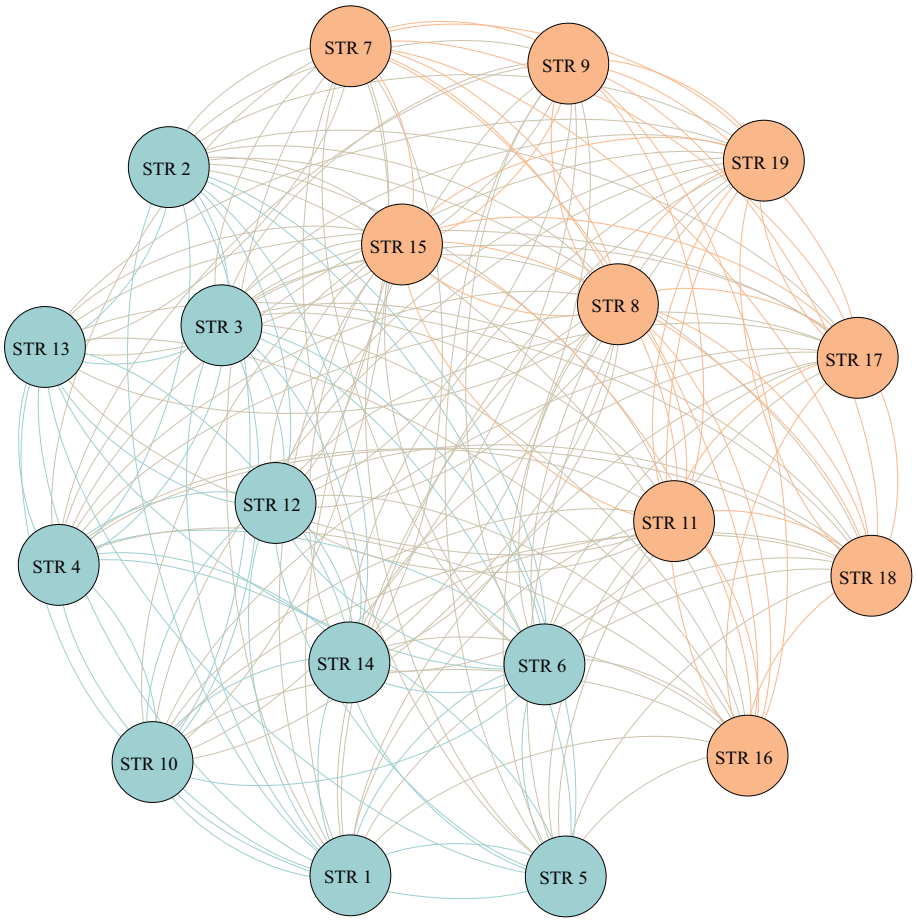

Figure 9 (Color online) Clusters of year 2019. Light blue: Group 1**; orange: Group 2**.

but not for fall ($p = 0.069$) and winter ($p = 0.946$). Group differences in the individual measurements of the TD, RD, and IRI were further investigated in the spring and summer seasons. The results show that the two groups differ in the RD measurement ($p < 0.05$) in spring but not for the other two seasons. In the summer season, the two groups differed significantly in terms of the TD value ($p < 0.05$), whereas the RD and IRI were not significantly different between the two groups. The individual measurements across the seasons in 2019 are shown in Figure 10.

3.5 Pavement performance analysis in 2020

Two groups were derived from the clustering method (Figure 11), with STRs 2–5, 7–11, 15, and 16 grouped together (Group 1***) and STRs 1, 6, 12–14, and 17–19 in the same group (Group 2***). Compared to

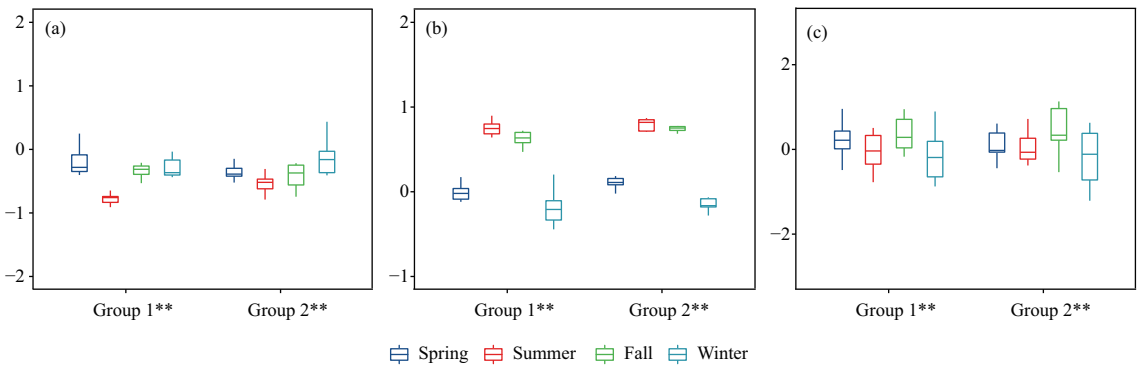

Figure 10 (Color online) Individual measurements in 2019 across seasons. (a) Texture depth across the four seasons and between the groups; (b) rutting depth; (c) IRI.

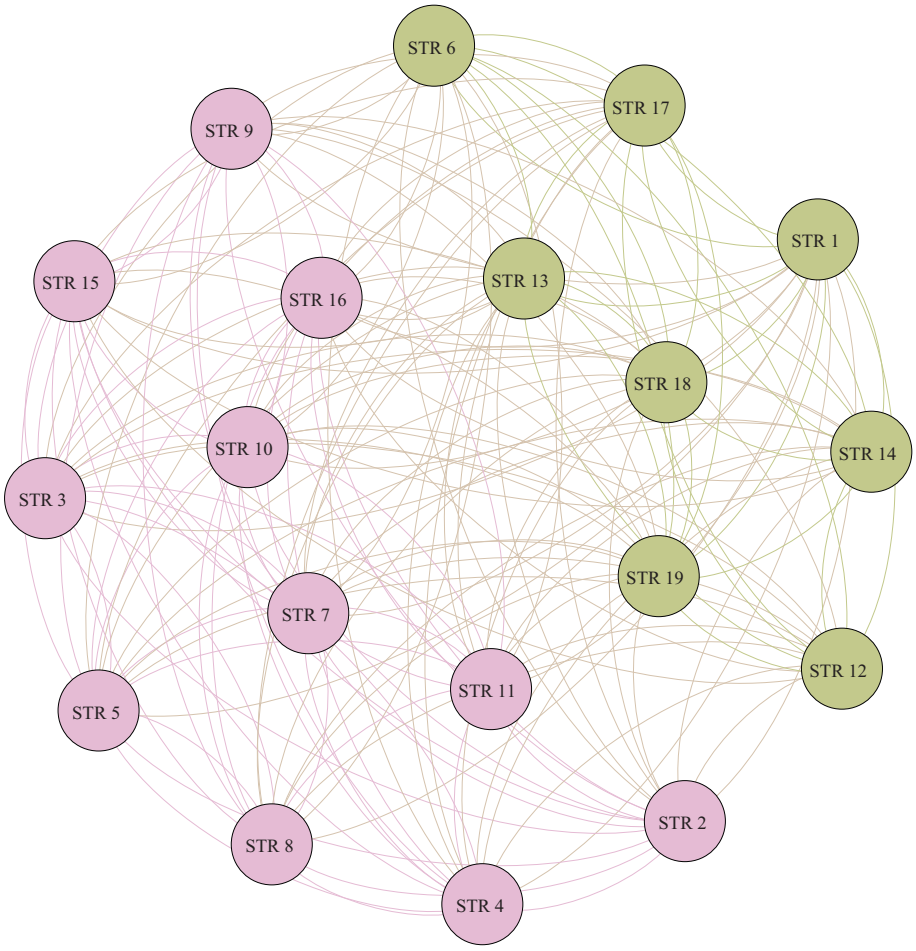

Figure 11 (Color online) Clusters of year 2020. Purple: Group 1^{***}; light green: Group 2^{***}.

the previous year, STRs 7–9, 11, and 17–19 maintained a similar performance and stayed in the same group, and STRs 2–5, 12, and 13 stayed together in other groups.

The statistics show the significant seasonal effect on the two groups ($p < 0.001$). The multivariate post-hoc comparisons reveal the significant differences between winter and summer ($p < 0.05$) and winter and fall ($p < 0.05$). The subsequent univariate comparisons display a significant TD measurement value between winter and fall ($p < 0.05$), and RD differs in both situations ($p < 0.001$). Furthermore, there is a significant group and season interaction effect on the combined pavement performance ($p < 0.001$). Specifically, the two groups differed in their performance in the summer season ($p < 0.05$), but no significant differences were found in the other three seasons. Finally, the group differences during the

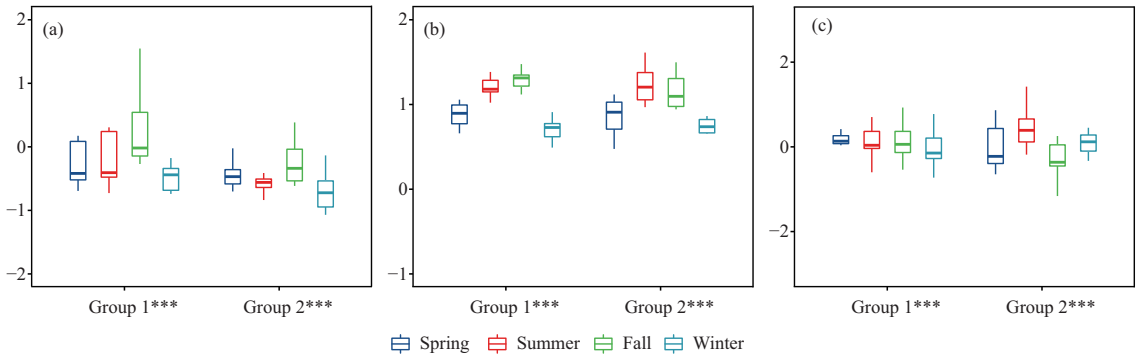

Figure 12 (Color online) Individual measurements in 2020 across seasons. (a) Texture depth across the four seasons and between the groups; (b) rutting depth; (c) IRI.

summer differed in the TD measurement ($p < 0.05$). Individual measurements across the seasons in 2020 are shown in Figure 12.

4 Discussion

The current study proposes a complex network approach for the evaluation of pavement performances among 19 structures. In particular, the TD, RD, and IRI pavement performances were submitted to the construction of the pavement performance network, and an unsupervised machine learning method was used for the clustering of pavement structures based on the pavement network. By comparing the proposed method with other state-of-the-art clustering methods, we demonstrated the effectiveness of the complex network approach in categorizing pavement structures.

To our knowledge, the current study is the first to use the complex network approach in delineating pavement structure profiles. This approach is particularly useful in fractionating the service performance of different types of pavement structures from a data-driven perspective. Our results add to the growing field in which network approaches are employed and demonstrate the profound application in understanding how clustering pavement structures might aid in a better understanding of pavement design and construction. In accordance with previous research in the literature, our results indicate a consistent seasonal change of pavement performance in each year of the experiment [38,39]. Particularly, pavement structures in our study displayed a smaller TD value during summer and fall, as compared to spring and winter. However, the pairwise comparison in 2017 is not significant. This result is in line with a study that used the Boltzmann fitting curve for temperature variations in the pavement TD, which shows a negative correlation between the TD and temperature of an asphalt surface [40]. In addition, an opposite pattern was revealed in the RD measurement, where a high temperature provides a high RD value. This is interpreted from previous research as increasing temperature influences the vertical strain in the pavement and subsequently results in the rutting damage [41].

Furthermore, the clustering analysis identified three groups in the first year of the experiment, showing the pavement performances in the short-term period. As expected, the groups were not significantly different from one another because all pavement structures operated by only approximately 3.7 million ESALs in the first year, which is equivalent to 2–4 years of service life in a real-world scenario. Within each group, overlapping and diversified design and construction between pavement structures could be observed. Specifically, the group with STRs 2, 8–11, 18, and 19 are categorized together. STRs 2, 8, and 9 are the common asphalt pavements, and STR 2 has thin AC. On the contrary, STRs 18 and 19 are the full-depth asphalt pavements, where the thickness of the AC layer reached 52 and 48 cm, respectively. Consequently, our results suggest that the thickness of the AC layer may not influence the pavement performance in a comparatively short period of time.

An analogous argument can be formulated with regard to the influence of the pavement thickness from the group containing STRs 3, 6, 7, 12, and 14–17. A common semi-rigid structure (i.e., STRs 6 and 7) showed a similar performance with a thick AC (i.e., STRs 14–17). However, different from the previous group, most of the pavement structures used high-strength subbase structures. Similar findings were found in the last group with STRs 1, 4, 5, and 13, where high-unconfined-compression-strength cement-bond-grade stones were used in the subbase. Therefore, based on the results, the strength of a

subbase structure affects the performance of the pavements. Furthermore, the results indicate a similar performance between rigid (i.e., STRs 4 and 5) and semi-rigid (i.e., STRs 1 and 13) structures. Based on the functional division of pavement structures, the rigid base structure shares a similar performance as the high-strength semi-rigid base structure [27]. The main difference between the two is that the stiffness of the semi-rigid base is significantly lower than that of the rigid base. Our results suggest a parallel pavement performance between the two structures, but it may only be applicable for a short period. In sum, the thickness of the AC may not affect the pavement performance in the short-term period. However, the performance can be differentiated based on the strength of the subbase structure from the observation in the first year.

A dramatic change in group allegiance emerged in the second year of the experiment, with 19 pavement structures divided into two groups instead of three. Based on the results, from the first year to the second year, the performance of the tested structures tended to be separated by the depth of the asphalt layers. Compared to the first year, STRs 2, 8–11, 18, and 19 stayed in the same group, with the new addition of STRs 15–17. The performance of STRs 15–17 converged to the full-depth asphalt base structure (i.e., STRs 18 and 19), despite these structures being built with comparatively thick asphalt layers (i.e., 36–52 cm). In the other groups, the structures were mainly constructed with a rigid/semi-rigid design composed of 12–28 cm asphalt layers. The effects of the asphalt layer thickness were investigated in previous research, and the results showed significant impacts on the pavement performance [42]. Our results further demonstrate that this influence may come later into the pavement performance than the subbase strength. In addition, STRs 12–14 were grouped together. All three structures, composed of 24 cm AC separated into three layers, have been frequently used in China in recent years. The main difference between the three structures is that the recycling materials were used in the lower AC layer in STR 14. The integration of waste and recycling materials into pavement design and construction has been proposed and tested in the past decades [43], but the exact service quality remains controversial [44]. Some previous studies have indicated that recycling materials are usually sensitive to temperature and moisture and hence temporally influence the performance [45]. In the current study, we indicate that recycling materials may not function differently than common pavement structures that are widely used in China. However, they differ from the thick AC structures after two years of accelerated testing.

The groups in the third year of the experiment started to show significant differences in the overall performance for each season. At this stage of the experiment, all pavement structures were conducted with approximately 22 million ESALs. It thus could be suggested that this amount of ESALs is a critical point for the service life of pavement structures. Accordingly, some studies have shown total cracks or thin surface cracks in pavement structures after approximately 10 million ESALs [46]. In the current study, cracks or fatigues were not yet observed. Nonetheless, one group (i.e., STRs 7–9, 11, and 15–19) displayed a slightly worse performance during spring and summer, as compared to the other groups. Specifically, the thin asphalt-based structure (i.e., STRs 1–3), rigid composite material (i.e., STRs 4 and 5), and inverted structure (i.e., STRs 10 and 12) showed superior performance than common semi-rigid-based pavement structures (i.e., STRs 7–9) and thick AC pavements (i.e., STRs 11, 15–19) in the comparatively high-temperature condition.

The results from the year 2020 suggest the categorization of pavement structures after a long term, such that 38 million ESALs are completed at the end of the year, which is equivalent to 12–15 years of service in real traffic. Corroborating previous findings [47], the performance of the full-depth AC pavement structure maintained a high standard in the long term. Thus, although the construction and maintenance cost of full-depth AC is comparatively higher than that of thin structures [48], the performance is indeed superior and stable. Furthermore, STRs 12–14 were grouped with full-depth AC in 2020. This result is not the case in the previous three years, and in fact, the performances were comparatively worse than those of full-depth AC pavements. An intriguing finding is that STR 14 used the recycling materials in the lower AC layer and showed an indiscriminate performance as those in the group. This finding may indicate the profound features of recycling materials used in the pavement layer.

In the other group, the thin semi-rigid (i.e., STRs 2, 3, and 7–9) and rigid composite structures (i.e., STRs 4 and 5) shared similar performance, as well as inverted (i.e., STR 10) and thick AC structures (i.e., STRs 11, 13, 15, and 16). These similarities were frequently observed during the four-year experiment period. Unexpectedly, these thick AC structures differ from full-depth AC in the long term. In particular, these thick AC structures use high-strength subbase materials like most of the other structures in this group, which results in the unstable performance in the long term, especially in the high-temperature season.

Nevertheless, a few limitations to the current study could potentially have masked the evaluation of asphalt pavement structures. The proposed approach to evaluate pavement structures requires comparatively large samples and extensive long-term experiments, which are usually not practical in other laboratories. Next, the proposed evaluation provides a broad overview of the similarity and/or diversity among 19 pavement structures in years, but it limited the analysis in the pairwise comparison. Recent advancements in computing methods could potentially be useful in the detailed analysis of pavement structures [49–51]. Finally, the analysis of our work is based on the measurements of the IRI, RD, and TD, but some other information could be examined in the future, such as pavement deflection and modulus.

5 Conclusion

In this paper, we propose a complex network approach to the evaluation of pavement performance. Specifically, we constructed a pavement structure network based on the similarity in performance testing. By utilizing an unsupervised machine learning technique, we clustered 19 pavement structures with diversified design and construction into separate groups in each year for the past four years (i.e., 2017–2020). Significant differences between the groups were detected using the bootstrapping-based repeated measure MANOVA. The results demonstrate the seasonal effect on pavement structures throughout the four years of the experiment. Furthermore, from the analysis of the 19 types of pavements, we indicate that the short-term pavement performances may not depend on the thickness of the AC but rely on the strength of the subbase structure. In addition, in the long term, the full-depth asphalt pavement structure showed stable high-standard performance. We indicate that the performances of pavement structures with recycling materials do not diverge from the full-depth AC structure but differ in the short-term period. Therefore, future research could focus on examining recycling materials, which may provide good long-term performance, be environmentally friendly, and have lower costs than traditional materials. In the meantime, the exact nature of the thickness of AC and subbase strength effect need an in-depth analysis to guide pavement construction and achieve outstanding performance.

Acknowledgements This work was supported in part by National Key Research & Development Project of China (Grant Nos. 2020YFA0714300, 2020YFA0714301) and National Natural Science Foundation of China (Grant Nos. 61833005, 61876036, 62003084)

References

1 Timm D H, Newcomb D E. Perpetual pavement design for flexible pavements in the US. Int J Pavement Eng, 2006, 7: 111–119
2 Hernando D, del Val M A. Guidelines for the design of semi-rigid long-life pavements. Int J Pavement Res Tech, 2016, 9: 121–127
3 Jamshidi A, White G. Evaluation of performance and challenges of use of waste materials in pavement construction: a critical review. Appl Sci, 2020, 10: 226
4 Barriera M, Pouget S, Lebental B, et al. In situ pavement monitoring: a review. Infrastructures, 2020, 5: 18
5 Yu J, Zhang X, Xiong C. A methodology for evaluating micro-surfacing treatment on asphalt pavement based on grey system models and grey rational degree theory. Constr Build Mater, 2017, 150: 214–226
6 Assogba O C, Tan Y, Zhou X, et al. Numerical investigation of the mechanical response of semi-rigid base asphalt pavement under traffic load and nonlinear temperature gradient effect. Constr Build Mater, 2020, 235: 117406
7 Reza B, Sadiq R, Hewage K. Emergy-based life cycle assessment (Em-LCA) for sustainability appraisal of infrastructure systems: a case study on paved roads. Clean Techn Environ Policy, 2014, 16: 251–266
8 Kodippily S, Tighe S L, Henning T F P, et al. Evaluating pavement performance through smart monitoring-effects of soil moisture, temperature and traffic. Road Mater Pavement Des, 2018, 19: 71–86
9 Yagi H, Yanagitani T, Numazawa T, et al. The physical properties of transparent $Y_3Al_5O_12$. Ceramics Int, 2007, 33: 711–714
10 Watson D K, Rajapakse R. Seasonal variation in material properties of a flexible pavement. Can J Civ Eng, 2000, 27: 44–54
11 Wang T H, Su L J, Zhai J Y. A case study on diurnal and seasonal variation in pavement temperature. Int J Pavement Eng, 2014, 15: 402–408
12 Alataş T, Yılmaz M, Kök B V, et al. Comparison of permanent deformation and fatigue resistance of hot mix asphalts prepared with the same performance grade binders. Constr Build Mater, 2012, 30: 66–72
13 Yu M, You Z, Wu G, et al. Measurement and modeling of skid resistance of asphalt pavement: a review. Constr Build Mater, 2020, 260: 119878
14 Chen L, Cong L, Dong Y, et al. Investigation of influential factors of tire/pavement noise: a multilevel Bayesian analysis of full-scale track testing data. Constr Build Mater, 2021, 270: 121484
15 Gong H, Sun Y, Shu X, et al. Use of random forests regression for predicting IRI of asphalt pavements. Constr Build Mater, 2018, 189: 890–897
16 Huffman J E. Full-depth pavement reclamation: state of the practice. J Assoc Asphalt Pav, 1997, 66: 746–759
17 Lane B, Kazmierowski T. Ten-year performance of full-depth reclamation with expanded asphalt stabilization on trans-Canada highway, Ontario, Canada. Transpation Res Record, 2012, 2306: 45–51
18 Jiang X, Zhang M, Xiao R, et al. An investigation of structural responses of inverted pavements by numerical approaches considering nonlinear stress-dependent properties of unbound aggregate layer. Constr Build Mater, 2021, 303: 124505
19 Li S, Fan M, Xu L, et al. Rutting performance of semi-rigid base pavement in RIOHTrack and laboratory evaluation. Front Mater, 2021, 7: 590604

20 AzariJafari H, Yahia A, Amor M B. Life cycle assessment of pavements: reviewing research challenges and opportunities. J Cleaner Production, 2016, 112: 2187–2197
21 White T D, Albers J M, Haddock S J E. Limiting design parameters for accelerated pavement testing system. J Transp Eng, 1992, 118: 787–804
22 Harvey J. Use of accelerated pavement testing to evaluate maintenance and pavement preservation treatments: introduction. Transp Res Circ, 2009, 139: 1–10
23 Kang H G, Zheng Y X, Cai Y C, et al. Regression analysis of actual measurement of temperature field distribution rules of asphalt pavement. China J Highw Transp, 2007, 20: 13–18
24 Huang W, Liang S M, Wei Y. Surface deflection-based reliability analysis of asphalt pavement design. Sci China Technol Sci, 2020, 63: 1824–1836
25 Ameri M, Mansourian A, Heidary Khavas M, et al. Cracked asphalt pavement under traffic loading—a 3D finite element analysis. Eng Fract Mech, 2011, 78: 1817–1826
26 Gao X, Wei Y, Huang W. Effect of individual phases on multiscale modeling mechanical properties of hardened cement paste. Constr Build Mater, 2017, 153: 25–35
27 Wang X D, Zhou G, Liu H, et al. Key points of RIOHTrack testing road design and construction. J Highway Transp Res Dev (Engl Ed), 2020, 14: 1–16
28 Zhang L, Zhou X, Wang X. Research progress of long-life asphalt pavement behavior based on the RIOHTrack full-scale accelerated loading test. Chin Sci Bull, 2020, 65: 3247–3258
29 Girvan M, Newman M E J. Community structure in social and biological networks. Proc Natl Acad Sci USA, 2002, 99: 7821–7826
30 Friedrich S, Brunner E, Pauly M. Permuting longitudinal data in spite of the dependencies. J Multivariate Anal, 2017, 153: 255–265
31 Bathke A C, Friedrich S, Pauly M, et al. Testing mean differences among groups: multivariate and repeated measures analysis with minimal assumptions. Multivariate Behaval Res, 2018, 53: 348–359
32 Konietschke F, Bathke A C, Harrar S W, et al. Parametric and nonparametric bootstrap methods for general MANOVA. J Multivariate Anal, 2015, 140: 291–301
33 Friedrich S, Pauly M. MATS: inference for potentially singular and heteroscedastic MANOVA. J Multivariate Anal, 2018, 165: 166–179
34 Ester M, Kriegel H P, Sander J, et al. A density-based algorithm for discovering clusters in large spatial databases with noise. In: Proceedings of the 2nd International Conference Knowledge Discovery and Data Mining, Portland, 1996. 96: 226–231
35 Ankerst M, Breunig M M, Kriegel H P, et al. Optics: ordering points to identify the clustering structure. SIGMOD Rec, 1999, 28: 49–60
36 Wu K L, Yang M S. Mean shift-based clustering. Patt Recogn, 2007, 40: 3035–3052
37 Wang K, Wang B, Peng L. CVAP: validation for cluster analyses. Data Sci J, 2009, 8: 88–93
38 García J A R, Castro M. Analysis of the temperature influence on flexible pavement deflection. Constr Build Mater, 2011, 25: 3530–3539
39 Nam B H, Yeon J H, Behring Z. Effect of daily temperature variations on the continuous deflection profiles of airfield jointed concrete pavements. Constr Build Mater, 2014, 73: 261–270
40 Wu J, Wang X D, Wang L, et al. Temperature correction and analysis of pavement skid resistance performance based on RIOHTrack full-scale track. Coatings, 2020, 10: 832
41 Zhao X, Shen A, Ma B. Temperature adaptability of asphalt pavement to high temperatures and significant temperature differences. Adv Mater Sci Eng, 2018, 2018: 1–16
42 Valle P D, Thom N. Pavement layer thickness variability evaluation and effect on performance life. Int J Pavement Eng, 2020, 21: 930–938
43 Zhang J, Ding L, Li F, et al. Recycled aggregates from construction and demolition wastes as alternative filling materials for highway subgrades in China. J Cleaner Production, 2020, 255: 120223
44 Canestrari F, Ingrassia L P. A review of top-down cracking in asphalt pavements: causes, models, experimental tools and future challenges. J Traffic Transp Eng, 2020, 7: 541–572
45 Vaitkus A, Gražulyte J, Baltrušaitis A, et al. Long-term performance of pavement structures with cold in-place recycled base course. Balt J Road Bridge Eng, 2021, 16: 48–65
46 Gao J, Yang J, Yu D, et al. Reducing the variability of multi-source reclaimed asphalt pavement materials: a practice in China. Constr Build Mater, 2021, 278: 122389
47 Dessouky S H, Al-Qadi I L, Yoo P J. Full-depth flexible pavement responses to different truck tyre geometry configurations. Int J Pavement Eng, 2014, 15: 512–520
48 Sakhaeifar M S, Brown E R, Tran N, et al. Evaluation of long-lasting perpetual asphalt pavement with life-cycle cost analysis. Transpation Res Record, 2013, 2368: 3–11
49 Farouk A, Batle J, Elhoseny M, et al. Robust general N user authentication scheme in a centralized quantum communication network via generalized GHZ states. Front Phys, 2018, 13: 1–8
50 Atia I, Salem M L, Elkholy A, et al. In-silico analysis of protein receptors contributing to SARS-COV-2 high infectivity. Inf Sci Lett, 2021, 10: 19
51 Zidan M, Abdel-Aty A, El-Sadek A, et al. Low-cost autonomous perceptron neural network inspired by quantum computation. AIP Conf Proc, 2017, 1905: 020005